Saturation and its effect on the resilient modulus of a pavement formation material

LETISHA BLACKMORE*, CHRISTOPHER R.I. CLAYTON†, WILLIAM POWRIE‡, JEFFREY A. PRIEST§ and LOUISE OTTER‖

This paper reports the effects of changing degree of saturation on the stiffness of a typical railway formation material. Material dynamically compacted to a target dry density over a range of water contents was cyclically loaded in triaxial and hollow cylinder apparatus. The results of both test types show the large effect of the degree of saturation on stiffness. In both the cyclic triaxial apparatus and the equivalent stress path in the cyclic hollow cylinder apparatus, the resilient modulus (M_R) increased considerably (from ~36 MPa to ~467 MPa) as the degree of saturation fell. M_R at a water content of 7% (optimum under the 2·5 kg rammer) was approximately 1·5 times the near-saturated value (at $w = 8\%$). M_R at the driest state tested ($w = 4\%$) was approximately 6 times that measured for the near-saturated specimen. In the hollow cylinder apparatus, these trends were seen regardless of whether principal stress rotation was applied. The increase in M_R associated with decreasing water content is thought to result from an increase in matric suction. Increased scatter in M_R at higher suction may be the result of a more variable distribution of water within drier specimens. Comparison of suction stresses derived from the soil water retention curve with values back-calculated from cyclic triaxial testing suggests that useful estimates of railway formation resilient modulus, M_R, may be made on the basis of measurements of matric suction.

KEYWORDS: laboratory tests; partial saturation; pavements & roads; repeated loading; stiffness; suction

INTRODUCTION

The design of granular railway formations and flexible highway pavements requires, among other things, knowledge of the stiffness of the layers of which they, and the underlying formation, are composed. The subgrade formation must provide a stable platform throughout its life, without failure or excessive deformation resulting from traffic-induced stresses, or the effects of changing environmental factors such as rainfall and evapotranspiration.

In the construction of a railway (or highway) the various pavement materials will be carefully selected and compacted in the field at optimum water content to achieve a specified dry density. It is, however, inevitable that target water contents will not be achieved precisely and that further changes in water content will occur during the life of the track structure. These will modify the behaviour of the materials and under unfavourable conditions may lead to poor track performance. This paper explores the effect of applied stresses and as-compacted water content on the resilient modulus (M_R) of a typical formation material.

Manuscript received 2 March 2018; revised manuscript accepted 5 March 2019.
Discussion on this paper is welcomed by the editor.

* Formerly University of Southampton, Southampton, UK; now University of Bath, Bath, UK.
† University of Southampton, Southampton, UK.
‡ University of Southampton, Southampton, UK (Orcid:0000-0002-2271-0826).
§ Formerly University of Southampton, Southampton, UK; now University of Calgary, Calgary, AB, Canada.
‖ Formerly University of Southampton, Southampton, UK.

MATERIAL TESTED

The material tested was a compacted clayey sand. It contained 11% by weight of clay and was made up from three grades of sand (Leighton Buzzard fractions B (46·5%), C (9·9%) and D (9·9%)), Oakamoor HPF5 silt (20·8%) and Hymod Prima ball clay (12·9%). The Hymod Prima ball clay (ECC, 2008) is commercially available and contains some quartz particles as well as clay. It was selected to represent sub-ballast layers typical of those used for new heavy-haul railway line construction, or for the upgrading of existing railway lines, such as the 580 km coal line in South Africa. It was termed material B by Gräbe & Clayton (2009).

The results of previous studies using this material have been reported by Gräbe & Clayton (2009, 2014), Otter *et al.* (2015) and Mamou *et al.* (2017, 2018). Table 1 compares plasticity test results (BS 1377 – part 4) for the material used in this study with those reported by Gräbe (2002) and Otter (2011).

In the field, during construction, the sub-ballast material is normally specified based on

(*a*) an acceptable particle size distribution
(*b*) compaction in the field at a moisture content close to the optimum water content (OMC), and
(*c*) achieving a dry density in the field greater than a specified value, based on the maximum dry density (MDD).

The OMC and MDD are determined in standard laboratory compaction tests as specified for example in the modified American Association of State Highway and Transportation Officials (AASHTO) T180 (AASHTO, 1993), ASTM D1557 (ASTM, 2007) and BS 1377-4 (BSI, 2012) 4·5 kg rammer tests.

The South African Transnet S410 earthworks specification (Transnet, 2006) distinguishes between four formation layers (SSB, SB, A and B) and bulk earthworks. The four formation

Table 1. Comparison of plasticity test results for material B fines with those reported by Gräbe (2002) and Otter (2011)

Study	Plastic limit: %	Liquid limit: %	Plasticity index: %	Clay content	Activity A
Gräbe (2002)	14	28	14	11	1·3
Otter (2011)	14	29	15	11	1·4
Present study	14	27	13	11	1·2

layers decrease in density and stiffness from the top down (SSB to layer B) and, in common with highway pavements, are prescribed to have sufficient stiffness and thickness to support the rail track and ballast over the design life. The minimum densities to be achieved in the field (in terms of the maximum dry density in the modified AASHTO laboratory compaction test) are 98%, 95%, 93% and 90%, respectively. Compaction water content in the field must be between +1% and −2% of the OMC in the same laboratory test.

SPECIMEN PREPARATION

The maximum dry density of material B was found from the BS 1377 4·5 kg rammer test to be 2·26 Mg/m^3 at an OMC of 4·8%, giving a target dry density in the field for type A formation of 2·15 Mg/m^3 and for type B formation of 2·10 Mg/m^3. Gräbe (2002) and Otter (2011) previously used a dry density of 2·10 Mg/m^3 for their laboratory testing. This value was adopted in the present study as it allowed a reasonable range of specimen water content to be tested and permitted the results of the different studies to be compared. The compaction energy needed to achieve the target dry density at each water content was found by trial and error.

Dry material was thoroughly mixed with the appropriate amount of water, by hand, in a sealed plastic bag and allowed to equilibrate for a minimum of 24 h. Solid 100 mm dia. specimens were compacted in a 204 mm high split mould, in five layers, using a pre-determined number of blows per layer. To improve axial uniformity the centres of the hollow cylinder apparatus (HCA) specimens were drilled out in two stages by hand using a wood auger, with an initial 30 mm dia. subsequently increased to 60 mm (the final internal diameter).

APPARATUS AND INSTRUMENTATION

The cyclic stiffness of a pavement or granular layer is an important parameter in the design of roads, runways and railways. Termed the 'resilient modulus', M_R, it is used as both a long-term and short-term performance prediction parameter (Khoury & Zaman, 2004). It is strongly affected by a number of factors, including material type, soil physical state (e.g. water content), normal effective stress, octahedral shear stress and stress history (e.g. type of loading and number of cycles of loading) (Li & Selig, 1996; Gräbe & Clayton, 2009). The suggestion that a single value of M_R might be used in flexible highway pavement design (AASHTO, 1993) has led to increased research (Lekarp *et al.*, 2000; Ceratti *et al.*, 2004; Ooi *et al.*, 2004; Liang *et al.*, 2008; Thom *et al.*, 2008; Cary & Zapata, 2011; Ng *et al.*, 2013; Salour & Erlingsson, 2015) on the effect of a number of these factors on M_R. Given the number of variables affecting M_R and their often wide ranges, complex test programmes are necessary to determine the likely variability of resilient modulus in any given project.

The cyclic triaxial apparatus (CTX) was adopted for this research. It has become increasingly used in advanced testing of pavement materials (Harrigan, 2004) and in research studies on the effect of water content on M_R (Cary & Zapata, 2011; Ng *et al.*, 2013; Salour & Erlingsson, 2015). The CTX readily enables a large number of specimens to be tested (Brown, 1996) so that the effects of cyclic loading of varying magnitudes, under a range of mean effective stresses, can be determined. However, the principal stress rotation (PSR) induced by a passing train (Powrie *et al.*, 2007) cannot be applied (Hight & Leroueil, 2003). Therefore, parallel tests were also conducted using a cyclic HCA (Gräbe & Clayton, 2009).

To ensure representative behaviour in an element test the minimum specimen dimension should not be smaller than the shear band thickness. The shear band thickness for granular materials has been estimated from laboratory observations as 10 times the maximum grain size (Roscoe, 1970; Muhlhaus & Vardoulakis, 1987) and as 7–8 times the mean grain size by Oda & Kazama (1998) from X-ray image analysis. The hollow cylinder specimens had a wall thickness of 20 mm, more than 10 times the 1·18 mm maximum particle size, allowing representative testing.

Because of the effect of suction (Otter *et al.*, 2015) high stiffness was expected even at the low net normal stresses that were to be applied. Therefore, to avoid bedding errors, specimens were fitted with local linear variable differential transformers (LVDTs) to measure radial and vertical strains over the middle third of the specimens. A detailed description of the LVDT set-up in the HCA is given by Gräbe & Clayton (2009). The use of local strain instrumentation was justified by the test results, global axial strain measurements being approximately 1·5 to 2 times the local strain measurements at OMC, and up to 7 times for drier, stiffer specimens tested in the CTX.

No pore water or air pressure measurements were made as the majority of the specimens were tested unsaturated. Measurement of pore pressures would have required slower rates of testing and the deployment of a tensiometer on the mid-plane. To mimic field conditions specimens were tested drained throughout – that is, the specimens were mounted on initially dry, low-air-entry porous stones and the air-filled back-pressure connection was vented to the atmosphere in a temperature-controlled room at 20°C. The matric suction could not therefore be controlled or measured during testing, but the pore air pressure was approximately atmospheric.

LOADING SEQUENCES

As noted above, M_R depends on several factors. The cyclic triaxial and hollow cylinder testing reported in this paper was used to investigate the effects of net normal stress, cyclic deviatoric stress and PSR on stiffness, for a single material, at a single dry density, and a range of specimen water contents.

Pavement materials operate at shallow depths. Overburden pressure is low and (relatively) large transient and cyclic normal and shear stresses are applied by the traffic, along with significant PSR. Typical confining pressures of 20, 40 and 100 kPa have been suggested for railway subgrade testing by Shahu *et al.* (2000), and in most of the pavement structure they can be expected to be less than 35 kPa (Miller *et al.*, 2000).

Network Rail (2005) uses the repeated load triaxial test apparatus to measure the undrained modulus of poorly performing subgrade, under a 30 kPa confining stress and a deviator stress of 30 kPa. However, this does not reflect the effects of different in situ depths or axle load variations.

The stress sequences applied during the CTX testing reported in this paper were based on the harmonised test method for flexible pavements as specified for granular subgrade material (Harrigan, 2004) following the recommendations of the National Cooperative Highway Research Program (NCHRP) project 1-28A, in which several AASHTO testing approaches were combined (harmonised). To cover the relevant ranges of the variables affecting M_R, each specimen was compacted at a target water content, w, before being subjected to a test sequence consisting of 20 loading stages as shown in Table 2. Each loading stage was conducted at one of five confining (cell) pressures ($p_o = 15$, 30, 40, 55 or 85 kPa), and for each confining pressure, deviator stress ratios (q_{cyc}/p_o) of 0·5, 1·0, 2·0 or 3·0 were applied, giving 20 stages in all. A minimum deviatoric stress (q_{min}) of 20% of the confining pressure was maintained throughout cycling, to ensure good contact between the specimen and the apparatus.

Taking stage number 3 in Table 2 as an example, the confining stress (cell pressure) was first increased from 30 kPa (applied during stage number 2) to 40 kPa. The minimum deviatoric stress was $0{\cdot}2 \times 40$ kPa = 8 kPa. For the desired cyclic stress ratio (q_{cyc}/p_o) of 0·5, the required cyclic deviatoric stress range (q_{cyc}) was 20 kPa. One hundred cycles of sinusoidal deviatoric stress were applied to the specimen, between 8 kPa and 28 kPa, about a cyclic stress datum of 18 kPa. The deviatoric stress was representative of the applied vertical stress from a passing train bogie, although it was applied at a somewhat slower rate, with a frequency in the CTX of 0·5 Hz.

Figure 1 shows total stress paths in the p–q plane during sinusoidal deviatoric stress cycling for the CTX test loading sequence in Table 2. The filled circular markers show the minimum stress points (q_{min}) for each of the five stress paths, resulting from the application of the cell pressure (15, 30, 40, 55 or 85 kPa) and a deviatoric stress of 20% of that cell pressure. The open, numbered markers represent the maximum stresses during cycling for each of the loading stages in Table 2, which had cyclic stress ratios of 0·5, 1·0, 2·0 and 3·0. No pre-conditioning was applied as this is considered unnecessary when local strain measurements are made (Nazarian *et al*., 1996) and may result in the underestimation of M_R (Cerni *et al*., 2015).

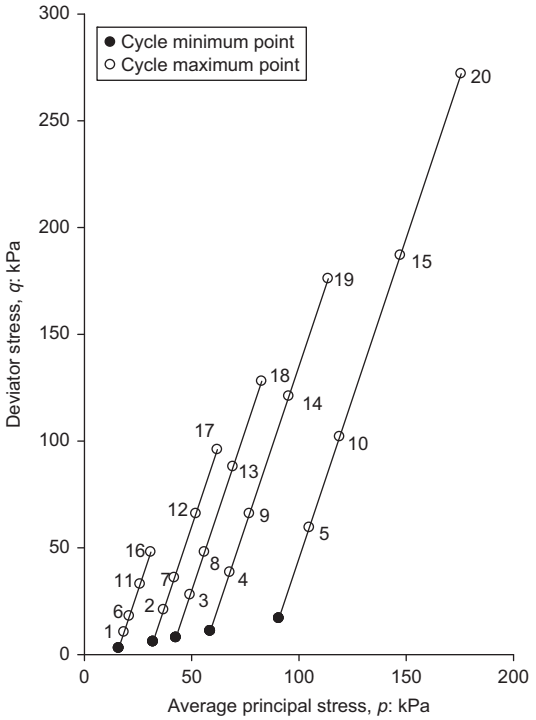

Fig. 1. Total stress paths during sinusoidal deviatoric stress cycling of cyclic triaxial test specimens

Table 2. CTX loading sequences based on the NCHRP project 1-28A – granular subgrade material test plan

CTX loading sequence	Confining pressure, p_o: kPa	Cyclic stress ratio (q_{cyc}/p_o)	Cyclic stress range, q_{cyc}: kPa	Cyclic stress datum: kPa
1	15	0·5	7·5	6·8
2	30	0·5	15	13·5
3	40	0·5	20	18·0
4	55	0·5	27·5	24·8
5	85	0·5	42·5	38·3
6	15	1·0	15	10·5
7	30	1·0	30	21·0
8	40	1·0	40	28·0
9	55	1·0	55	38·5
10	85	1·0	85	59·5
11	15	2·0	30	18·0
12	30	2·0	60	36·0
13	40	2·0	80	48·0
14	55	2·0	110	66·0
15	85	2·0	170	102·0
16	15	3·0	45	25·5
17	30	3·0	90	51·0
18	40	3·0	120	68·0
19	55	3·0	165	93·5
20	85	3·0	255	144·5

Figure 2 shows typical CTX results during cycling for loading sequence number 7. Fig. 2(a) shows the development of global and average local vertical strain over 100 cycles at 0·5 Hz. M_R was calculated using the average of the recoverable local strain measurements made on diametrically opposite sides of the specimen unless stated otherwise. Deviator stress is plotted against vertical strain for cycles 1–5 and cycles 95–100 in Fig. 2(c). The straight line between the minimum and maximum points of cycle 100 indicates the basis of calculating resilient modulus, which is the slope of this line. Fig. 2(b) shows the total stress path under which the specimen was loaded cyclically.

The preparation of specimens and the stress paths applied in the HCA were broadly similar to those in the CTX.

(*a*) Specimens were prepared by compaction at a range of water contents to a target dry density of 2·10 Mg/m^3.
(*b*) The expected total stress path experienced by a representative element in the track foundation was applied.
(*c*) Matric suction was not measured and it was assumed that there was negligible pore air pressure during cycling; thus the net normal stress was equated to the applied total stress.

The effect of PSR on the measured resilient modulus was investigated by applying stages of loading with and without PSR. The cyclic stresses applied by Gräbe (2002) to simulate train-induced stresses were used during this study, to check

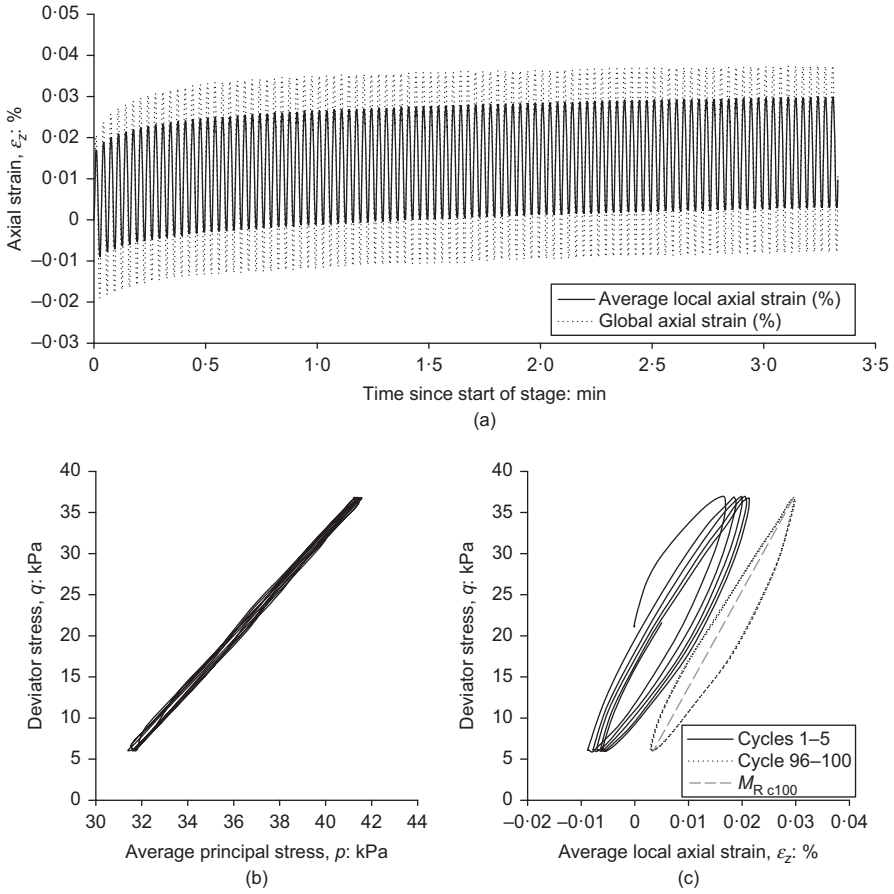

Fig. 2. Typical CTX results during cycling. (a) Development of global and local strains with time when loaded at 30 cycles/min. (b) Deviator stress, q, plotted against average total principal stress, p. (c) Deviator stress, q, as a function of vertical local strain, for selected cycles, showing calculation of M_R

repeatability. Fig. 3 shows the two cyclic stress paths in terms of the applied stresses.

(*a*) In stress path 1 (SP1), the specimen was subjected to a cyclic axial (deviatoric) stress while the inner and outer cell pressures were held constant. No torsional load was applied so that there was no shear stress on the horizontal plane of the specimen, equivalent to loading in the CTX (sequence 7).
(*b*) In stress path 2 (SP2), the specimen was subjected to both cyclic deviatoric and cyclic torsional loading, thus inducing PSR. The inner and outer cell pressures were held constant and the cyclic rotational loading was 90° out of phase with the cyclic deviator stress.

Because of the added complexity of torsional loading, a more restricted set of loading conditions was applied during HCA testing. An average confining pressure, p_o, of 30 kPa was selected to represent the pressures due to self-weight in a typical railway formation following Miller *et al.* (2000) and Shahu *et al.* (2000). A constant ratio of cyclic deviatoric stress (q_{cyc}) to confining stress (p_o) of 1·0 was adopted in the HCA tests, as in sequence number 7 of the CTX testing (see Table 2). This was selected to be well below the expected failure stress ratio for materials compacted in a well-designed pavement.

The frequency of cycling applied in the HCA was 0·017 Hz (a period of 1 min), much slower than applied in the CTX (0·5 Hz) and expected in the field, which might be up to at least 3 Hz for a high-speed railway (3·26 Hz being the vehicle passing frequency for a Valero train having an axle spacing of 2·5 m travelling at 80 m/s; (Milne *et al.*, 2017)), or 13 Hz if individual wheel loading dominates. Limitations of data acquisition and control software prevented faster cycling in the HCA. The lower rate of cycling is likely to have reduced any build-up of excess pore air pressures or pore water pressures and consequent changes in net normal stress and matric suction. The influence of the slower testing rate on the measured resilient modulus was considered small based on comparisons of M_R measured in the HCA and CTX. A discussion of the influence of cyclic loading frequency and drainage conditions is given in Mamou *et al.* (2017).

Each of the HCA tests consisted of four phases. First, an isotropic confining stress of 30 kPa was applied to equilibrate the specimen under in situ stress conditions. This was followed by three cyclic loading phases. Phases 1 and 3 applied 500 cycles of SP2 (no PSR, see above). Phase 2 applied 1000 cycles of SP1 (with PSR), except in test HCA + 0v2 for which the stress path order was changed (nl. stress path version 2 (v2)). This approach was adopted to allow an assessment of the effects of staging sequence (see Table 3). The first part of each test name (e.g. 'HCA' or 'CTX') denotes the apparatus used to obtain the data. This is followed by a number (e.g. '-3') denoting the specimen's water content relative to optimum. The stress path adopted for the majority of testing was termed 'version 1' (or 'v1') leading to a test name such as HCA-1·7v1. Other test variants (v0 and v2) examined, for example, the effect of test stage sequences.

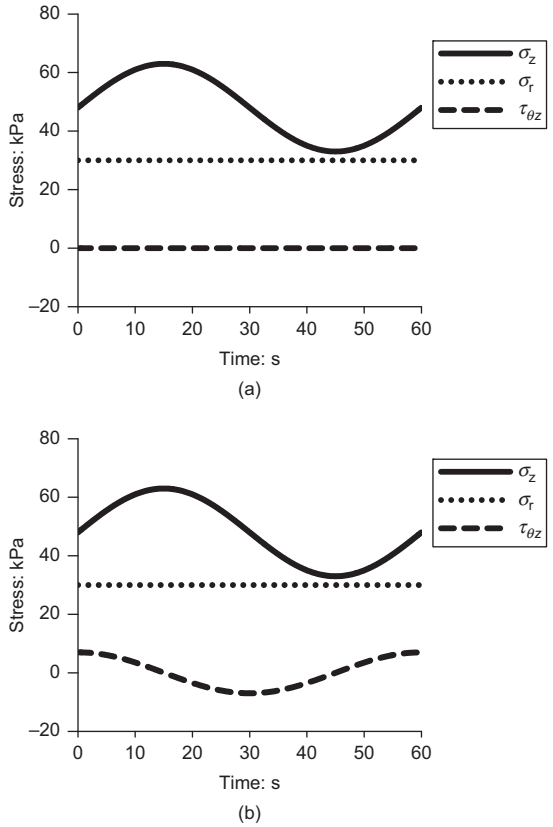

Fig. 3. Cyclic stress paths applied in the HCA in terms of the applied stresses σ_z, $\sigma_r = \sigma_\theta$ and $\tau_{\theta z}$ to investigate the effect of PSR on M_R (redrawn from Gräbe (2002)). (a) SP1 without PSR and (b) SP2 with PSR

Table 3. Cyclic loading with and without PSR used in the HCA testing

Test name	HCA loading sequence		
	Cyclic test phase	Cyclic stress path	Number of cycles
HCA + 0v1	1	SP2	500
	2	SP1	1000
	3	SP2	500
HCA + 0v2	1	SP1	500
	2	SP2	1000
	3	SP1	500
HCA-1v1	1	SP2	500
	2	SP1	1000
	3	SP2	500
HCA-1·7v1	1	SP2	500
	2	SP1	540*
HCA-2v1	1	SP2	500
	2	SP1	1000
	3	SP2	120*
HCA-3iv1	1	SP2	500
	2	SP1	1000
	3	SP2	500
HCA-3iiv1	1	SP2	500
	2	SP1	1000
	3	SP2	500
HCA + 1v1	1	SP2	500
	2	SP1	1000
	3	SP2	500

Note: During PSR, confining stress = 30 kPa, deviatoric stress amplitude = 7 kPa, datum = 0 kPa, phase angle = 90°.
*Test interrupted.

Loading rate and drainage

The resilient modulus, M_R, of each specimen was determined from the average strains measured in both the CTX and the HCA from the last five cycles up to the 100th cycle of deviatoric stress loading. However, the cyclic frequency used in the CTX was 0·5 Hz in line with the NCHRP project 1-28A testing protocol, whereas in the HCA a lower frequency of one cycle per minute (0·0167 Hz) was necessary to facilitate data logging and maintain test control.

The time required between the different test stages is not prescribed in the NCHRP project 1-28A. Initially, testing was conducted allowing a rest period of 5 min following each cell pressure increase and 10 min following each cell pressure decrease (from 85 kPa to 15 kPa at the beginning of stages 6, 11 and 16). For each loading stage, the deviator stress datum ($q_{min} + q_{cyc}/2$) was initially changed to its next value over a period of 2 min, but this was adjusted after it was found that this gave inadequate time for pore pressure dissipation in specimens with higher water contents. Subsequent testing applied cell pressure changes at a rate of 2 kPa/min.

Stress history effects

The stiffness of a railway formation, as with soil, is known to be influenced by its stress history. Gräbe (2002) explored the effect of overconsolidation ratio (OCR) on saturated formation material consolidated from a slurry. He found that M_R increased by about 20% when the OCR was increased from 15 to 25, and that the application of PSR had relatively little influence (a few per cent) on the effect of OCR.

In the tests reported in this paper the specimens were for the most part unsaturated and dynamically compacted, and therefore did not require pre-conditioning by overconsolidation. However, the effect of multi-staging in the CTX needed to be assessed since formation materials cannot be assumed to behave elastically; hence stiffness cannot be assumed to be solely dependent on material type, water content and stress state. The effect of CTX multi-staging on the measured stiffness was investigated by changing the loading sequence from that described in Table 2. These tests showed that the sequence of loading stages did not significantly influence the measured values of M_R provided vertical strains remained below 5%.

TYPICAL RESULTS

Figure 2 shows typical CTX results during cycling a specimen with a water content of 7% under loading sequence 7. Fig. 2(a) shows the development of global (external) and local strains during the application of 100 cycles of sinusoidal deviatoric stress loading. The significant differences in amplitude between these two sets of results suggest that resilient modulus must be measured using local strain instrumentation. Fig. 2(b) shows the stress path during cycling. Fig. 2(c) shows deviatoric stress plotted as a function of local vertical strain for the first five and the last five loading cycles. Despite the hysteresis, 100 cycles were sufficient to produce a stable (resilient) stress–strain behaviour in this material, at these stress levels. The slope of the straight line joining the two ends of the final hysteretic loop shows the position at which the resilient modulus was measured.

Figure 4 shows resilient modulus measured in the CTX apparatus as a function of confining pressure, p_o (Fig. 4(a)), and maximum deviator stress, q_{max} (Fig. 4(b)), for water contents between 4 and 8%. Reducing the water content has the dominant effect although increases in p_o and q_{max} also lead to more modest increases in M_R.

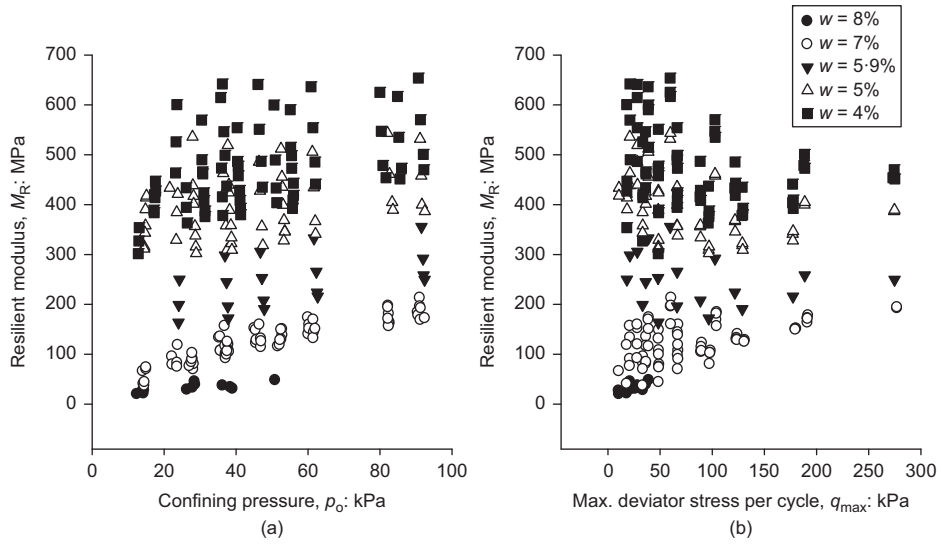

Fig. 4. Measured resilient modulus from CTX tests for specimens at various water contents as a function of (a) of confining stress, p_o, and (b) maximum deviator stress, q_{max}

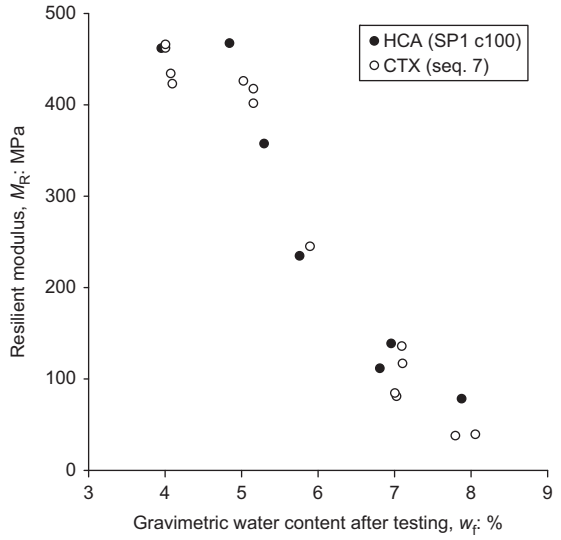

Fig. 5. Comparison of resilient modulus measured in the cyclic triaxial test and in the HCA under CTX conditions

DISCUSSION

Resilient moduli (M_R) obtained from the cyclic triaxial (CTX) and hollow cylinder (HCA) tests on unsaturated clayey sand reported in this paper are broadly in line with the relatively few results reported in the literature for low-plasticity soils. M_R values for specimens with a water content of 7% and a dry density of 2·10 Mg/m^3 were between 110 and 150 MPa, similar to those back-figured from field monitoring in South Africa reported by Gräbe *et al.* (2005) and Priest *et al.* (2010). The track subgrade resilient modulus design target value adopted for this material in South Africa is typically 100 MPa (Lourens & Maree, 1997; Gräbe, personal communication, 2017).

Effect of apparatus type

Figure 5 compares resilient moduli measured at the end of load sequence number 7 in the CTX at a range of water contents with those measured in the HCA under cyclic triaxial conditions (SP1 at cycle 100). Despite some scatter the results show reasonable agreement between the two different methods over the range of water contents tested.

A smaller difference between the values of axial strain measured on radially opposite sides of the specimen was seen in the HCA than in the CTX. This could be a result of differences between the load cell arrangement and specimen fixity in each apparatus (Baldi *et al.*, 1988; Gasparre *et al.*, 2014). The HCA axial/torque load cell is integrated with the top cap fitted to the specimen to allow rotational loading, while the load cell in the CTX is not fixed to the top cap. The CTX load cell is integrated into a ram with hemispherical end placed onto a coned seating, such that a slight eccentricity of load onto the specimen top cap can be accommodated (Baldi *et al.*, 1988; Gasparre *et al.*, 2014).

Effect of water content and degree of saturation

The HCA and CTX measurements of stiffness (M_R) in general confirm the large effect of water content and degree of saturation (Fig. 5) on stiffness previously seen by Otter *et al.* (2015) at very small strains in resonant column (RCA) tests. Fig. 5 indicates a maximum resilient modulus in the order of 450 MPa at water contents between 4 and 5% suggesting that stiffness of this material may peak or even decrease at water contents less than 5%. At a water content of 8% (close to saturation) the measured resilient modulus in the CTX tests is approximately one order of magnitude lower than the maximum values. At low net normal stresses Otter and co-workers measured a tripling in G_0, from ∼50 MPa to ∼150 MPa, as the degree of saturation reduced from near saturated to approximately 55% ($w = 5\%$). In the present study a decrease in water content resulted in an up to six-fold increase in M_R (Fig. 6) compared to the near-saturated value (at $w = 8\%$), although part of this increase may be a result of the higher strains in the HCA and CTX tests than in the RCA. The M_R value measured for the near-saturated specimen (at $w = 8\%$) of HCA + 1v1 was selected as representative of the saturated response in the context of values from tests conducted by Gräbe (2002) on the same material prepared from slurry. The permanent strains, measured after 500 cycles on low-water-content specimens, were significantly smaller (approximately 0·002% for $w = 4\%$ and $w = 5\%$) than at a higher water content (0·17% at OMC = 7%). For comparison, the G_0 values reported by Otter *et al.* (2015) were measured at shear strains of less than 0·001%.

The M_R increased considerably, from 36·4 to 467 MPa (Fig. 5), as the degree of saturation decreased from 85 to 45%

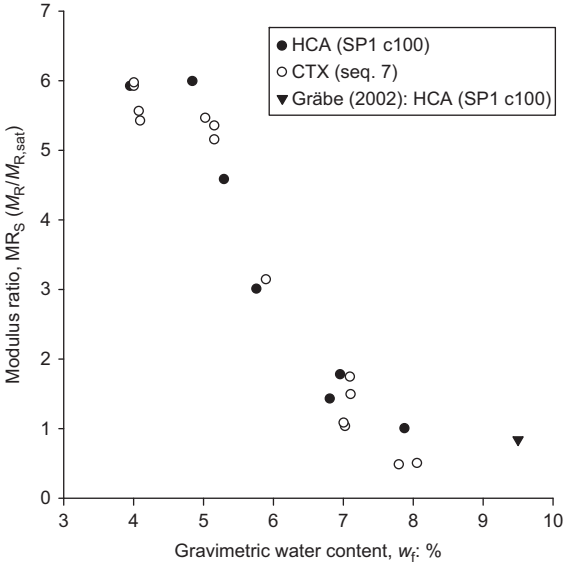

Fig. 6. Suction modulus ratio (MR_S) indicating the relative change in M_R due to a change in water content (and associated suction) of the material. HCA and CTX M_R normalised by $M_{R,sat}$ (HCA + 1v1). Value from Gräbe (2002) included for comparison only

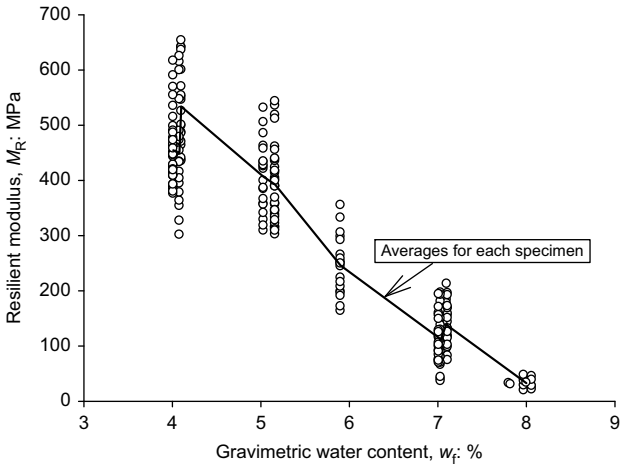

Fig. 7. Resilient modulus as a function of final water content, w_f for all tests and sequences

when measured in the CTX and equivalent HCA (SP1) tests carried out with $p_o = q_{cyc} = 30$ kPa at different compaction water contents (between $w = 8\%$ and $w = 4\%$). The average M_R at optimum ($w = 7\%$) was approximately 1·7 times the near-saturated value (at $w = 8\%$) from HCA test results. M_R at the driest state tested ($w = 4\%$) was approximately 6 times the value measured for the near-saturated specimen. The scatter in M_R for all tests decreased significantly as the water content increased (Fig. 7). This is a result of a number of factors that affect M_R on this plot, which are discussed in the following sections. There was a significant proportional decrease in average resilient modulus as the water content increased, particularly from optimum (7%) towards saturation.

Effect of confining pressure (p_o) and cyclic/maximum deviator stress (q_{cyc}/q_{max})

Figure 4 shows the effects of confining pressure (p_o) and cyclic/maximum deviator stress (q_{cyc}/q_{max}) on the resilient modulus, M_R, measured during the 100th cycle of loading for different water contents. Confining pressures varied from 15 to 85 kPa, and cyclic deviator stresses from 7·5 to 255 kPa. Comparing the trends in the resilient moduli determined for specimens with 8% water content with those for specimens with lower water contents shows that although confining pressure and cyclic deviator stress have a significant effect on M_R, the effect of water content (hence degree of saturation) dominates for water contents greater than 5%. This is confirmed in Fig. 7.

In some cases, the stresses applied to the formation by traffic appear to have a more significant influence on the resilient modulus. Fig. 4(a) shows M_R as a function of p_o for water contents, w_f. At a water content of 7% (optimum) there is a clear, non-linear trend of M_R increasing with p_o. Although there appears to be a similar underlying trend at 4% water content, this is largely obscured by scatter in the data. This may be a result of inadequate instrument resolution at the very high specimen stiffnesses associated with small water contents. It could also be related to the water content within the sample becoming more variable (or random) at lower water contents as it relates to the small pore spaces (Alonso *et al.*, 2013). Any effects of q_{cyc} and q_{max} on M_R are obscured by this scatter in the data.

Effect of permanent strain

An increase in M_R with decreasing water content may have been to some extent the result of lower permanent strains, since the tests in the CTX and HCA were stress controlled. The permanent strains measured after 500 cycles were significantly smaller for low water content (approximately 0·002% for $w = 4\%$ and $w = 5\%$) than for higher water content specimens (0·17% at OMC = 7%).

Effect of drainage during cyclic loading

All testing was carried out drained (for both air and water) by allowing the top and bottom pore pressure lines to drain to the atmosphere. It was assumed that the pore air pressure in the specimens remained at atmospheric ($u_a = 0$), giving a net normal stress, $\sigma_n = \sigma - u_a$, equal to the applied total stresses. Variations in matric suction during cyclic loading were not assessed.

For specimens tested wet of optimum ($w = 8\%$) and close to saturation ($S_r > 95\%$) M_R measured in the CTX was considerably lower (in the order of half) than measured in the HCA. This is thought to have been due to a build-up of excess pore pressure in the CTX, although in the absence of mid-plane pore pressure measurement this hypothesis could not be tested. In contrast, comparable values of M_R were obtained for unsaturated (lower water content) specimens tested in the CTX and the HCA after 100 cycles with $p_o = q_{cyc} = 30$ kPa, without PSR (Fig. 5).

Effect of principal stress rotation

The effect of PSR on the resilient modulus was investigated using the HCA, applying identical stages of normal stress loading with and without PSR as already described. The cyclic stresses used by Gräbe (2002) to simulate train loading were applied (Table 3).

Figure 8 shows the effects of water content (and inferred suction through the soil water retention curve (SWRC)) on the ratio of M_R measured, using the HCA, with PSR (SP2) and without PSR (SP1) ($MR_{PSR} = M_{R,SP1}/M_{R,SP2}$), for each water content specimen as measured after 500 and 1000 cycles, respectively. The modulus ratio at OMC ($w = 7\%$) was approximately 1·15, representing a 13% reduction in M_R when PSR was applied. Thus at OMC M_R will be slightly overestimated if measured in the CTX without PSR. Fig. 8

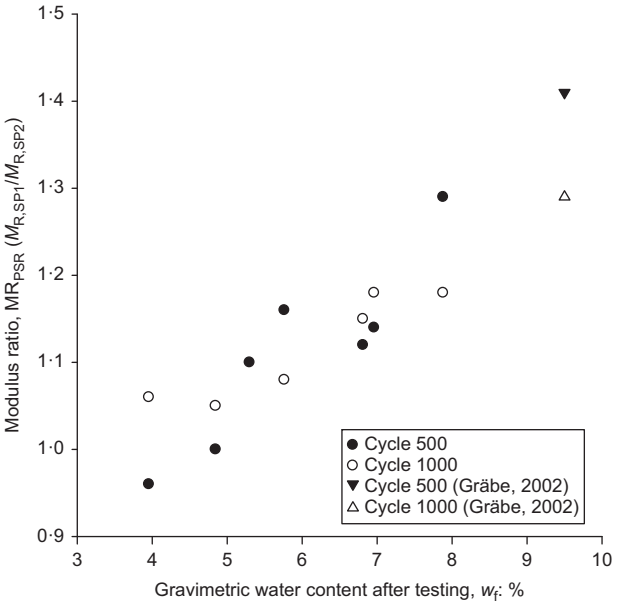

Fig. 8. Effect of PSR (SP2 in the HCA) on resilient modulus (e.g. $MR_{PSR,c500} = M_{R,SP1,c500}/M_{R,SP2,c500}$) at different water contents (hence suctions)

shows that MR_{PSR} decreases as the water content (and hence stiffness, M_R) decreases. In practical terms, given the difficulties of measurement, the effect of PSR on the stiffness of unsaturated pavement formation can therefore reasonably be ignored for the typical load case considered.

Effect of suction

It is not possible to express the effective stress of an unsaturated soil in terms of its pore water pressure, or indeed any single parameter, because the pore water is discontinuous and the liquid and air phases of the pore fluid require (at least) two independent state variables. A number of simplified approaches to the determination of an equivalent effective stress for an unsaturated material have been proposed in recent years.

To assess the effect of suction on rail formation stiffness the 'suction stress' approach (Lu & Likos, 2006; Lu *et al.*, 2010) was adopted as follows.

(*a*) First, the matric suction or SWRC for material B was calculated from data presented by Otter (2011) using the curve fitting procedure by Fredlund & Xing (1994), with their correction factor, $C(\psi)$.
(*b*) The suction stress (σ_s) was then obtained by multiplying the calculated matric suction by the effective degree of saturation (Alonso *et al.*, 2013), to produce the suction stress characteristic curve (SSCC).

The SWRC, for the material B also tested in the present study, was derived by Otter (2011) using Chandler's filter paper method (Chandler *et al.*, 1992). Otter (2011) carried out a large number of tests on material B. She found the air entry value and residual water content difficult to identify, which made determination of the inflexion point on the SWRC uncertain.

Otter (2011) fitted her SWRC data using Fredlund and Xing's (1994) equation

$$\theta_w = \frac{\theta_s}{\left\{\ln\left[e + \left(\frac{\psi}{a}\right)^n\right]\right\}^m} \quad (1)$$

with its correction factor

$$\theta = \theta_w C(\psi) \quad (2)$$

where

$$C(\psi) = \frac{\ln(1 + \psi/\psi_r)}{\ln[1 + (1\,000\,000/\psi_r)]} \quad (3)$$

θ_w is the volumetric water content at matric suction, ψ; θ_s is the saturated volumetric water content (taken as 20·4% in this case); e is Euler's number (2·71828); ψ_r is the residual matric suction; and determined the Fredlund and Xing variables as $a = 150$ kPa, $n = 1{\cdot}1841$ and $m = 0{\cdot}92327$.

Lu *et al.* (2010) proposed that the suction stress, σ_s, represents the contribution of suction (considered as particle contact level forces (Santamarina, 2003; Mitchell & Soga, 2005) to the effective stress governing the shear strength of unsaturated soil. Here and in Otter *et al.* (2015) the concept has been extended to stiffness, relating the suction stress at any water content to the matric suction by the effective degree of saturation, S_e, defined by Lu *et al.* (2010) as

$$\sigma_s = -\frac{\theta - \theta_r}{\theta_s - \theta_r}(u_a - u_w) = -S_e(u_a - u_w) \quad (4)$$

where θ is the volumetric water content; θ_r is the residual volumetric water content; and θ_s is the saturated volumetric water content.

The calculated SWRC for material B is shown as a dashed line in Fig. 9 for a dry density of 2·1 Mg/m^3 as determined previously by Otter (2011) and Otter *et al.* (2015) for the same material tested in this study. The matric suction varies from zero at saturation ($w = 9{\cdot}8\%$) to approximately 800 kPa at a water content of 4%.

Otter (2011) identified the residual matric suction as 1500 kPa at a water content of 3%. The matric suction from the SWRC was multiplied by the effective degree of saturation, S_e, to obtain the SSCCs. To assess the effect of the residual water content selected, the SSCC was also calculated

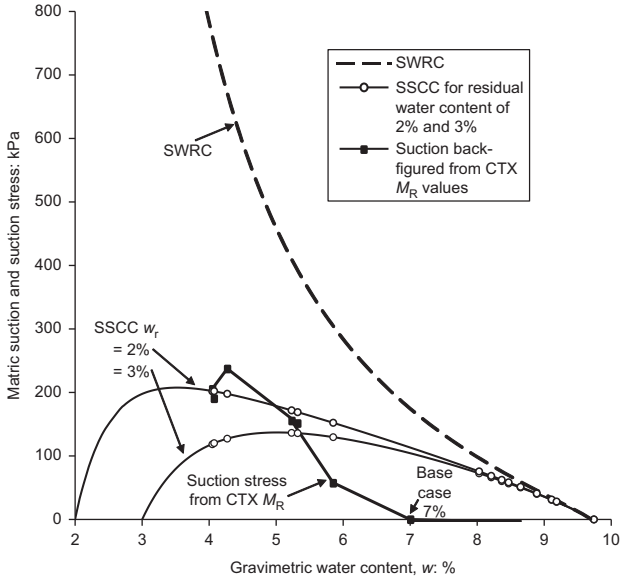

Fig. 9. Suction stress estimated from the SWRC for residual water contents of 2% and 3%, compared with values back-calculated from cyclic triaxial M_R results for material B compacted at optimum water content (7%)

for a residual water content of 2%. The SSCCs for the two residual water contents are shown by the thin full lines in Fig. 9. The suction stress (σ_s) is then added to the net normal stress (σ_n) to obtain the 'equivalent effective stress'. Note that a reduction in suction stress at low water contents, as seen in Fig. 9, can be expected in granular materials (Lu & Likos, 2006), as the impact of the small amounts of water remaining becomes negligible as the soil dries.

The open circles superimposed on the SSCC curves represent the water contents and the calculated suction stresses, based on the SSCC, of the specimens tested in the CTX. For specimens with gravimetric water contents dry of optimum (in the range 4–5·5%) Fig. 9 shows that the suction stresses are expected to be between about 120 and 210 kPa. These are much greater than the net normal stresses of 15 to 85 kPa imposed during testing, indicating the significance of suctions in increasing the resilient modulus. The group of results at water contents greater than 7% represents specimens made up at or wet of optimum, and close to saturation. The suction stresses calculated from the SSCC for gravimetric water contents between 8 and 9·2% (S_R between 82·1 and 94·5%) range from approximately 50 to 70 kPa. However, it should be emphasised that the SSCC refers to specimens of the particular density for which the SWRC on which it is based applies.

Suction stresses (σ_s) were also back-calculated from the M_R results for specimens at different water contents using the approach suggested by Heath *et al.* (2004). Multi-variate linear regression analysis was applied to optimise the correlation between measured and calculated M_R for the OMC specimen according to the 'universal model' (Uzan, 1985; Lekarp *et al.*, 2000) to determine the three parameters, k_1, k_2 and k_3, in equation (5)

$$M_R = k_1 p_a \left(\frac{\Theta}{p_a}\right)^{k_2} \left(\frac{\tau_{oct}}{p_a} + 1\right)^{k_3} \quad (5)$$

where Θ is the bulk effective stress, the sum of the principal effective stresses ($\sigma'_1 + \sigma'_2 + \sigma'_3$); τ_{oct} is the octahedral shear stress $\left(= \left(\sqrt{2}/3\right)(\sigma'_1 - \sigma'_3)\right)$ for triaxial compression; p_a is atmospheric pressure (100 kPa); and k_1, k_2, k_3 are regression coefficients.

The back-calculation method uses the regression coefficients determined from the cyclic triaxial test on material compacted at OMC (in this case, 7%) as the base case, given that this test was completed within the 5% vertical strain limit specified by Harrigan (2004). Equation (5) was then used to determine the mean principal stress (p) required to obtain an M_R value in a test on a hypothetical base case specimen (OMC) equal to that measured in each of the unsaturated specimens. The suction stress for each unsaturated specimen was then calculated from the difference between this value of p_o and the value of p_o actually applied during the test. Twenty M_R values were determined from each of the CTX tests of which approximately 5% of the total of 200 measurements were excluded from the regression analysis as outliers. The results from the 'equivalent M_R' approach are shown in Fig. 9 by filled square markers connected by straight lines.

In contrast to the suction stress at OMC of ~100 kPa based on the SSCC, in taking the test on material compacted at OMC as the base case in the equivalent M_R calculation, it is inherently assumed that suction stresses do not contribute to the stiffness response at or above OMC. For the material tested in this study this was considered reasonable; during CTX testing the OMC specimen suffered volumetric strain which, although within the limits prescribed by Harrigan (2004), likely led to an increase in the degree of saturation (and in dry density) and a decrease in suction stress. Test specimens compacted above OMC were excluded from the sample set owing to their large axial strains (reaching the strain limits prescribed by Harrigan (2004) within three out of a total of 20 test stages), which made them not strictly comparable. As a result, zero suction stresses were assumed in specimens compacted at or wet of optimum for the purpose of back-calculating the suction stress using the equivalent M_R method. It is recommended that, in general, the selection and interpretation of the base case results consider the volumetric strain measured and implied changes in degree of saturation (dry density) that occur during CTX testing. Unfortunately, no matric suction measurements were made on materials after CTX testing.

The σ_s values back-calculated from the CTX results are compared with those estimated from the SSCC in Fig. 9. Except for those at a water content of 5·8% these values are in reasonable agreement especially in view of the assumptions adopted in the methodologies. For materials dry of optimum, a residual water content of 2% gives a better fit with the back-calculated values than a residual water content of 3%. Further work is required to explore the suction stresses developed at water contents close to optimum.

It should be noted that the suction stress approach by Lu & Likos (2006) is conceptual only. Although the results appear promising care should be taken in adopting the suction stress method without further research to assess the effects of

(*a*) the non-uniqueness of the SWRC and the influence of scanning curves (Fredlund *et al.*, 2002)
(*b*) the difficulty in identifying key elements of the SWRC, for example, the residual water content and inflection point, which needs to be overcome (Otter, 2011)
(*c*) the accuracy with which water content can be measured; all the work described in this paper was carried out over a very limited range of water content (4 to 8%), such that the impact of small changes or errors is amplified
(*d*) the need for local strain measurement to avoid the very significant effects of bedding on M_R associated with the very high stiffness at low water contents
(*e*) the non-linear behaviour of pavement materials and the resulting influence of using linear regression analyses to extrapolate M_R values from OMC when calculating suction stress values from cyclic triaxial values.

CONCLUSIONS

(*a*) Values of residual modulus M_R obtained from CTX and HCA tests on the unsaturated clayey sand reported in this paper are broadly in line with the relatively few values reported in the literature for low-plasticity soils of this type. M_R measured at optimum water content, OMC, ($w = 7\%$), was between 110 MPa and 150 MPa, similar to values back-figured from field monitoring in South Africa reported by Gräbe *et al.* (2005) and by Priest *et al.* (2010).
(*b*) M_R increased considerably, from 36 to 467 MPa, as the degree of saturation of the specimens decreased from 95 to 45%, when measured in CTX tests and equivalent HCA (SP1) tests carried out with $p_o = q_{cyc} = 30$ kPa.
(*c*) The HCA and CTX results reported in this paper in general confirm the large effect of degree of saturation on stiffness previously noted by Otter (2011) and Otter *et al.* (2015) from very small strain (G_0) resonant column testing. Otter *et al.* (2015) measured a tripling in G_0 when the degree of saturation reduced from near saturated to approximately 55% ($w = 5\%$). In this study, the stiffness (M_R) measured in the CTX and HCA

increased by a factor of about 6 as the degree of saturation decreased to about 45%.

(*d*) Previous laboratory measurements of resilient modulus have sometimes been made under saturated conditions. These will significantly underestimate the field values likely to be achieved after placement at OMC (S_R approximately 85%) and maximum dry density.

(*e*) Smaller water content changes, similar to those that might be expected when compacting under construction equipment within given tolerances, also led to significant changes in measured resilient modulus. The average M_R at optimum ($w = 7\%$) was approximately 1·7 times the near-saturated value (at $w = 8\%$).

(*f*) Otter *et al*. (2015) observed a peak in stiffness at a water content of about 5%. The present authors' data are not inconsistent with the idea of a peak at 4·5% water content, or at least a plateau for materials tested dry of 5%.

(*g*) At least part of the increase in stiffness (M_R) measured at lower water contents in the CTX and HCA tests may have been a consequence of reducing strains under constant applied stress paths. The permanent strains, measured after 500 cycles on low-water-content specimens were significantly smaller (approximately 0·002% for $w = 4\%$ and $w = 5\%$) than at higher water content (0·17% at OMC = 7%).

(*h*) The suction stress approach shows promise as a means of estimating the matrix stiffness of rail formation materials. However, at this stage the semi-empirical nature of the method and the practical difficulties in determining the SWRC should be borne in mind as potential limitations.

ACKNOWLEDGEMENTS

The work described in this paper was funded by the Engineering and Physical Science Research Council (EPSRC) through the Programme Grants Track 21 project (EP/H044949/1) and Track to the Future (EP/M025276/1); and Network Rail through the Strategic University Partnership with the University of Southampton in Future Infrastructure Systems. All data supporting this study are openly available from the University of Southampton repository at dx.doi.org/10·5258/SOTON/D0830.

NOTATION

k_n	regression coefficient
M_R	resilient modulus
N	number of load cycles
P	period
p	mean principal stress
p_a	atmospheric pressure
p_o	external (confining) cell pressure
q	deviator stress
q_{cyc}	cyclic deviator stress or maximum deviator stress difference
q_{max}	maximum deviator stress
q_{min}	minimum deviator stress
S_e	effective degree of saturation
S_r	degree of saturation
u_a	pore air pressure
w	gravimetric water content
w_f	gravimetric water content after testing
w_i	compaction gravimetric water content
w_r	residual gravimetric water content
ε_R	recoverable (elastic) strain
Θ	bulk stress (total stress)
θ	volumetric water content
θ_r	residual volumetric water content
θ_S	saturated volumetric water content
σ	total stress
σ_n	net normal stress
σ_s	suction stress
σ_1	major principal stress
σ_2	intermediate principal stress
σ_3	minor principal stress
τ_{oct}	octahedral shear stress
ψ	total suction
ψ_m	matric suction
ψ_r	residual matric suction

REFERENCES

AASHTO (American Association of State Highway and Transportation Officials) (1993). *AASHTO guide for design of pavement structures*, 4th edn. Washington, DC, USA: American Association of State Highway and Transportation Officials.

Alonso, E. E., Pinyol, N. M. & Gens, A. (2013). Compacted soil behaviour; initial state, structure and constitutive modelling. *Géotechnique* **63**, No. 6, 134, https://doi.org/10.1680/geot.11.P.134.

ASTM (2007). ASTM D1557-07: Standard test method for laboratory compaction characteristics of soil using modified effort. West Conshohocken, PA, USA: ASTM International.

Baldi, G., Hight, D. W. & Thomas, G. E. (1988). A reevaluation of conventional triaxial test methods. In *Advanced triaxial testing of soil and rock* (eds R. T. Donaghe, R. C. Chaney and M. L. Silver), ASTM STP 977, pp. 219–263. Philadelphia, PA, USA: American Society for Testing and Materials.

Brown, S. F. (1996). Soil mechanics in pavement engineering. *Géotechnique* **46**, No. 3, 383–426, https://doi.org/10.1680/geot.1996.46.3.383.

BSI (2012). BS 1377: Methods of test for soils for civil engineering purposes. London, UK: BSI.

Cary, C. E. & Zapata, C. E. (2011). Resilient modulus for unsaturated unbound materials. *Road Mater. Pavement Des.* **12**, No. 3, 615–638.

Ceratti, J. A., Gehling, W. Y. & Nunez, W. P. (2004). Seasonal variation of a subgrade soil resilient modulus in southern Brazil. *Transpn Res. Rec.* **1874**, 165–173.

Cerni, G., Corradini, A., Pasquini, E. & Cardone, F. (2015). Resilient behaviour of unbound granular materials through repeated load triaxial test: influence of the conditioning stress. *Road Mater. Pavement Des.* **16**, No. 1, 70–88.

Chandler, R. J., Crilly, M. S. & Montogomery-Smith, G. (1992). A low-cost method of assessing clay desiccation for low-rise building. *Proc. Instn Civ. Engrs – Civ. Engng* **92**, No. 2, 82–89, https://doi.org/10.1680/icien.1992.18771.

ECC (2008). *Hymod Prima product specification. C1/323/B*, 5th edn. Par, UK: ECC, IMERYS Minerals Ltd. See https://www.imerys-oilfieldsolutions.com/index.php/ball-clay (accessed 03/04/2019).

Fredlund, D. G. & Xing, A. (1994). Equations for the soil-water characteristic curve. *Can. Geotech. J.* **31**, No. 3, 521–532.

Fredlund, M. D., Wilson, G. W. & Fredlund, D. G. (2002). Use of the grain-size distribution for estimation of the soil-water characteristic curve. *Can. Geotech. J.* **39**, No. 5, 1103–1117, https://doi.org/10.1139/t02-049.

Gasparre, A., Hight, D. W., Coop, M. R. & Jardine, R. J. (2014). The laboratory measurement and interpretation of small-strain stiffness of stiff clay. *Géotechnique* **64**, No. 12, 942–953, https://doi.org/10.1680/geot.13.P.227.

Gräbe, P. J. (2002). *Resilient and permanent deformation of railway foundations under principal stress rotation*. Southampton, UK: University of Southampton.

Gräbe, P. J. & Clayton, C. R. (2009). Effects of principal stress rotation on permanent deformation in rail track foundations. *J. Geotech. Geoenviron. Engng* **135**, No. 4, 555–565.

Gräbe, P. J. & Clayton, C. R. (2014). Effects of principal stress rotation on resilient behavior in rail track foundations. *J. Geotech. Geoenviron. Engng* **140**, No. 2, 04013010.

Gräbe, P. J., Clayton, C. R. & Shaw, F. J. (2005). Deformation measurement on a heavy haul track formation. In *Proceedings of the 8th international heavy haul conference*, pp. 287–295. Rio de Janeiro, Brazil: International Heavy Haul Association.

Harrigan, E. T. (2004). Laboratory determination of resilient modulus for flexible pavement design. *NCHRP Res. Results Dig.* **285**, https://doi.org/10.17226/21960.

Heath, A. C., Pestana, J. M., Harvey, J. T. & Bejerano, M. O. (2004). Normalizing behavior of unsaturated granular pavement materials. *J. Geotech. Geoenviron. Engng* **130**, No. 9, 896–904.

Hight, D. W. & Leroueil, S. (2003). Characterisation of soils for engineering purposes. In *Characterisation and engineering properties of natural soils* (eds T. S. Tan, K. K. Phoon, D. W. Hight and S. Leroueil), pp. 255–362. Lisse, the Netherlands: Swets & Zeitlinger.

Khoury, N. N. & Zaman, M. M. (2004). Correlation between resilient modulus, moisture variation, and soil suction for subgrade soils. *Transpn Res. Rec.* **1874**, 99–107.

Lekarp, F., Isacsson, U. & Dawson, A. (2000). State of the art. I: Resilient response of unbound aggregates. *J. Transpn Engng* **126**, No. 1, 66–75.

Li, D. & Selig, E. T. (1996). Cumulative plastic deformation for fine-grained subgrade soils. *J. Geotech. Engng* **122**, No. 12, 1006–1013.

Liang, R. Y., Rabab'ah, S. & Khasawneh, M. (2008). Predicting moisture-dependent resilient modulus of cohesive soils using soil suction concept. *J. Transpn Engng* **134**, No. 1, 34–40.

Lourens, J. P. & Maree, J. S. (1997). Rehabilitation design of high embankments and a coal track formation. In *Proceedings of the 6th international heavy haul conference*, vol. 1, pp. 57–75. Cape Town, South Africa: International Heavy Haul Association.

Lu, N. & Likos, W. J. (2006). Suction stress characteristic curve for unsaturated soil. *J. Geotech. Geoenviron. Engng* **132**, No. 2, 131–142.

Lu, N., Godt, J. W. & Wu, D. T. (2010). A closed-form equation for effective stress in unsaturated soil. *Wat. Resour. Res.* **46**, No. 5, W05515, https://doi.org/10.1029/2009WR008646.

Mamou, A., Powrie, W., Priest, J. A. & Clayton, C. R. (2017). The effects of drainage on the behaviour of railway track foundation materials during cyclic loading. *Géotechnique* **67**, No. 10, 845–854, https://doi.org/10.1680/jgeot.15.P.278.

Mamou, A., Priest, J. A., Clayton, C. R. & Powrie, W. (2018). Behaviour of saturated railway track foundation materials during undrained cyclic loading. *Can. Geotech. J.* **55**, No. 5, 689–697.

Miller, G. A., Li, D. & Zaman, M. M. (2000). Cyclic shear strength of soft railroad subgrade. *J. Geotech. Geoenviron. Engng* **126**, No. 2, 139–147.

Milne, D. R., LePen, L. M., Thompson, D. J. & Powrie, W. (2017). Properties of train load frequencies and their applications. *J. Sound Vibr.* **397**, 123–140, https://doi.org/10.1016/j.jsv.2017.03.006.

Mitchell, J. K. & Soga, K. (2005). *Fundamentals of soil behavior*, 3rd edn. Hoboken, NJ, USA: John Wiley & Sons Inc.

Muhlhaus, H. B. & Vardoulakis, I. (1987). The thickness of shear bands in granular materials. *Géotechnique* **37**, No. 3, 271–283, https://doi.org/10.1680/geot.1987.37.3.271.

Nazarian, S., Pezo, R. & Picornell, M. (1996). *Testing methodology for resilient modulus of base materials*, Research report 1336-1. El Paso, TX, USA: Center for Geotechnical and Highway Materials Research.

Ng, C. W., Zhou, C., Yuan, Q. & Xu, J. (2013). Resilient modulus of unsaturated subgrade soil: experimental and theoretical investigations. *Can. Geotech. J.* **50**, No. 2, 223–232, https://doi.org/10.1139/cgj-2012-0052.

Network Rail (2005). *Business process document NR/SP/TRK/9039 formation treatment*. London, UK: Network Rail.

Oda, M. & Kazama, H. (1998). Microstructure of shear bands and its relation to the mechanisms of dilatancy and failure of dense granular soils. *Géotechnique* **48**, No. 4, 465–481, https://doi.org/10.1680/geot.1998.48.4.465.

Ooi, P. S., Archilla, A. R. & Sandefur, K. G. (2004). Resilient modulus models for compacted cohesive soils. *Transpn Res. Rec.* **1874**, 115–124.

Otter, L. (2011). *The influence of suction changes on the stiffness of railway formation*. Southampton, UK: University of Southampton.

Otter, L., Clayton, C. R., Priest, J. A. & Gräbe, P. J. (2015). The stiffness of unsaturated railway formations. *Proc. Instn Mech. Engrs, Part F: J. Rail Rapid Transit* **230**, No. 4, 1040–1052.

Powrie, W., Yang, L. A. & Clayton, C. R. (2007). Stress changes in the ground below ballasted railway track during train passage. *Proc. Instn Mech. Engrs, Part F: J. Rail Rapid Transit* **221**, No. 2, 247–261.

Priest, J. A., Powrie, W., Yang, L. A., Gräbe, P. J. & Clayton, C. R. I. (2010). Measurements of transient ground movements below a ballasted railway line. *Géotechnique* **60**, No. 9, 667–677, https://doi.org/10.1680/geot.7.00172.

Roscoe, K. H. (1970). The influence of strains in soil mechanics. *Géotechnique* **20**, No. 2, 129–170, https://doi.org/10.1680/geot.1970.20.2.129.

Salour, F. & Erlingsson, S. (2015). Resilient modulus modelling of unsaturated subgrade soils: laboratory investigation of silty sand subgrade. *Road Mater. Pavement Des.* **16**, No. 3, 553–568.

Santamarina, J. C. (2003). Soil behaviour: the role of particle shape. In *Soil behavior and soft ground construction* (eds J. T. Germaine, T. C. Sheahan and R. V. Whitman), pp. 25–56. Reston, VA, USA: American Society of Civil Engineers.

Shahu, J. T., Yudhbir, & Kameswara, R. (2000). A rational method for design of railroad track foundation. *Soils Found. – Jap. Geotech. Soc.* **40**, No. 6, 1–10.

Thom, R., Sivakumar, V., Brown, J. & Hughes, D. (2008). A simple triaxial system for evaluating the performance of unsaturated soils under repeated loading. *Geotech. Testing J.* **31**, No. 2, 107–114.

Transnet (2006). *S410: Specifications for railway earthworks*. Johannesburg, South Africa: Transnet Freight Rail (previously Spoornet), a division of Transnet Limited.

Uzan, J. (1985). Characterization of granular material. *Transpn Res. Rec.* **1022**, 52–59.